Supporting Information

1. Modelling of droplet detachment

According to the analysis above, the saturation of contact angle serves as the critical condition of the detachment of droplet. This can be explained by the energy balance between the electric energy stored in the EDL E_{c-o}, viscous dissipation E_{visc} and kinetic energy E_k. In this case, the difference of surface energy before/after removing the E-field is not considered because it is presented in the form of energy stored in EDL. Therefore, the following equation is obtained:

$$E_{c-o} = E_{visc} + E_k \qquad \text{(S-1)}$$

The E_{C-O} is given by the energy stored in the EDL. In general, the capacitance of the EDL is the combination of two capacitances in serial, i.e., the Helmholtz layer and diffusion layer[1]. However, in our study, the size of the droplet is far smaller than the Debye length under pH ~ 7 (~ tens of nm). In addition, as is observed in Fig.4, the molecules close to the surface (~ 2.5 Å) is significantly influenced by the E-field while those beyond the Helmholtz layer mainly remain not affected. Therefore, it is reasonable to simplify the capacitance as follow given the linear drop of voltage in this layer:

$$E_{c-o} = \frac{1}{2} C_H V^2 \qquad \text{(S-2)}$$

Where V is the applied voltage and C_H is the capacitance of the Helmholtz layer with an area and gap of A and d, which is expressed by:

$$C_H = \frac{\varepsilon \varepsilon_0}{d} A \qquad \text{(S-3)}$$

The thermodynamic limit for the saturation of EWOD is derived by Quinn et al[2] from the Young-Lippmann's equation as:

$$\cos \ddot{\theta} = \cos \theta_0 + \frac{C_H}{2\gamma} \ddot{V}^2 \qquad \text{(S-4)}$$

Where $\ddot{\theta}$ and θ_0 are denoted as the saturated contact angle and initial contact angle without E-field, respectively. $\ddot{V}$ is the critical voltage that leads to the saturation of

contact angle. γ is the interfacial tension at the liquid/gas interface.

Rearranging the Eq. S-2 to S-4 gives

$$E_{c-o} = \gamma(\cos\dot{\theta} - \cos\theta_0) \qquad \text{(S-5)}$$

The viscous dissipation during the contraction of droplet is derived by Chandra et al[3]

$$E_{visc} = \frac{3}{8}\frac{We}{Re}\beta^4\pi d_{in}\gamma \qquad \text{(S-6)}$$

Where We and Re are the Weber and Reynold numbers in terms of the center of mass during the contraction process. β is the ratio between the minimum and maximum diameters of droplet.

The critical condition is given according to $E_{c-o} = E_{visc}$:

$$\cos\dot{\theta} = \frac{3}{8}\frac{We}{Re}\beta^4\pi d_{in} + \cos\theta_0 \qquad \text{(S-7)}$$

The above equation gives the critical condition to judge whether a droplet can detach from the surface after removing the E-field. If the contact angle is not reached, the electric energy fails to compensate the viscous dissipation during the contraction process, and thus the droplet fails to detach as shown for the case $\delta = 0.05\ e$ and 0.08 e for $\varepsilon_{c-o} = 0.012$ kcal/mol. If addition, increasing the initial wettability (i.e., with a smaller θ_0) decreases the saturated angle, which complies with the observation, e.g., the saturation angle decreases from $\sim 30°$ to $\sim16°$ as the ε_{c-o} increases from 0.012 to 0.036 kcal/mol.

Although the viscous dissipation is the critical condition, there is no viscous dissipation as long as the droplet can detach as observed in Fig.2 because the stretched droplet rebounds without contraction. In this case, the electric energy almost completely converts into the kinetic energy, which is comprised of the translational motion of the center of mass and oscillation of the droplet from the stretched state to the round-shape. The translational kinetic energy for the droplet is

$$E_k^{tr} = \frac{1}{12}\rho_l v_{com}^2 \pi d_{in}^3 \qquad \text{(S-8)}$$

Considering an inviscid liquid droplet, the oscillating frequency can be obtained by

equating the rate of change for the perturbation, radial gradient for the velocity potential for the droplet and that for the surrounding fluid, which is subject to the second mode as described in Ref[4].

$$\omega_{osc}^2 = \frac{8\gamma}{\rho_l R^3} \qquad \text{(S-9)}$$

And the elastic coefficient of the droplet is calculated by $\omega_{osc} = \sqrt{2k_{osc}/m}$ and given as follows

$$k_{osc} = \frac{4\pi\gamma}{\rho_l} \qquad \text{(S-10)}$$

Assuming that the displacements for the compressed and stretched states are the same, with the EWOD state as the compressed state while the round-shape as the equilibrium state, the oscillatory amplitude A_{osc} can be calculated as:

$$A_{osc} = \frac{d_{in}}{2}\left[1 - \beta(1 - \cos\overset{\cdot\cdot}{\theta})\right] \qquad \text{(S-11)}$$

Replacing the saturated contact angle with $\overset{\cdot\cdot}{\theta} = arccos\dfrac{\gamma_c}{\gamma}^2$ gives

$$A_{osc} = \frac{d_{in}}{2}\left[1 - \beta(1 - \frac{\gamma_c}{\gamma})\right] \qquad \text{(S-12)}$$

where γ_c is the critical surface tension as defined by Zisman[5]

Therefore, the oscillatory kinetic energy is calculated according to $E_{osc} = \frac{1}{2}k_{osc}A_{osc}^2$

$$E_{osc} = \frac{\pi\gamma d_{in}^2}{2\rho_l}\left[1 - \beta(1 - \frac{\gamma_c}{\gamma})\right]^2 \qquad \text{(S-13)}$$

Combining the equation Eq. 11-15 and letting $E_k^{tr} = E_{c-o} - E_{osc}$ leads to

$$v_{com}^2 = \frac{12}{\pi\gamma d_{in}^3}\left[E_{c-o} - \frac{\pi\gamma d_{in}^2}{2\rho_l}\left[1 - \beta(1 - \frac{\gamma_c}{\gamma})\right]^2\right] \qquad \text{(S-14)}$$

It can be learned from SI Eq.14 that with given initial wettability and physical properties, the velocity of droplet obeys the $v_{com}^2 \sim E_{c-o}$ law as correlated in Eq.2 in

manuscript. The $v_{com}^2 \sim E_{c\text{-}o}$ law, in turn, indicates that there is little viscous dissipation during the detachment of droplet, which, otherwise, will introduce a linear term as shown in Eq.S-6 above due to the term $\dfrac{We}{Re} \sim v_{com}$.

2. **Observation of droplet detachment with different *E*-field at $\varepsilon_{c\text{-}o}$ = 0.012 kcal/mol**

   Fig.S1 shows the dynamics response of droplet after removing the *E*-field, corresponding to Fig.2 d to e. It can be seen that for all cases where the droplet detaches ($\delta \geq$ 0.15 *e*) there is no retraction of droplet over the surface, and thus there is no viscous dissipation. The droplet fails to detach below the critical *E*-field where the saturated contact angle is not reached. The videos for δ = 0.05 *e* and 0.5 *e* are also given in the attachment.
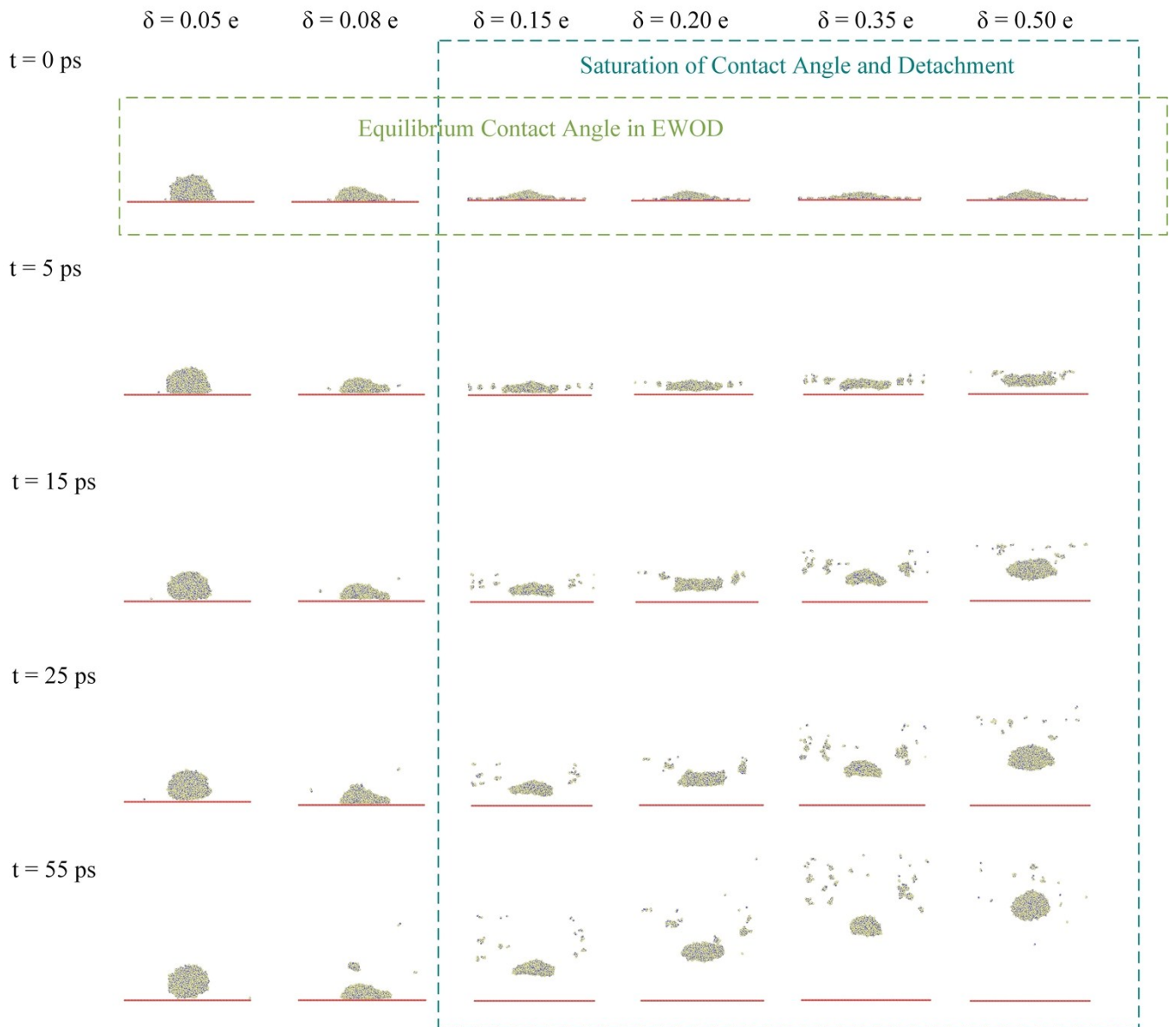
Fig.S1. Screen shots of droplet movement after removing the E-field with variation in the E-field. (Corresponding to Fig.2d to e)

3. Observation of droplet detachment with different initial wettability at $\delta = 0.5$ e

Fig.S2 shows the droplet movement after removing the E-field with different ε_{c-o}, which is in correspondence to Fig.3. Droplet jumps for $\varepsilon_{c-o} \leq$ 33E-3kcal/mol. The droplet detaches without retraction as well. The droplet height decreases with increase of ε_{c-o}.
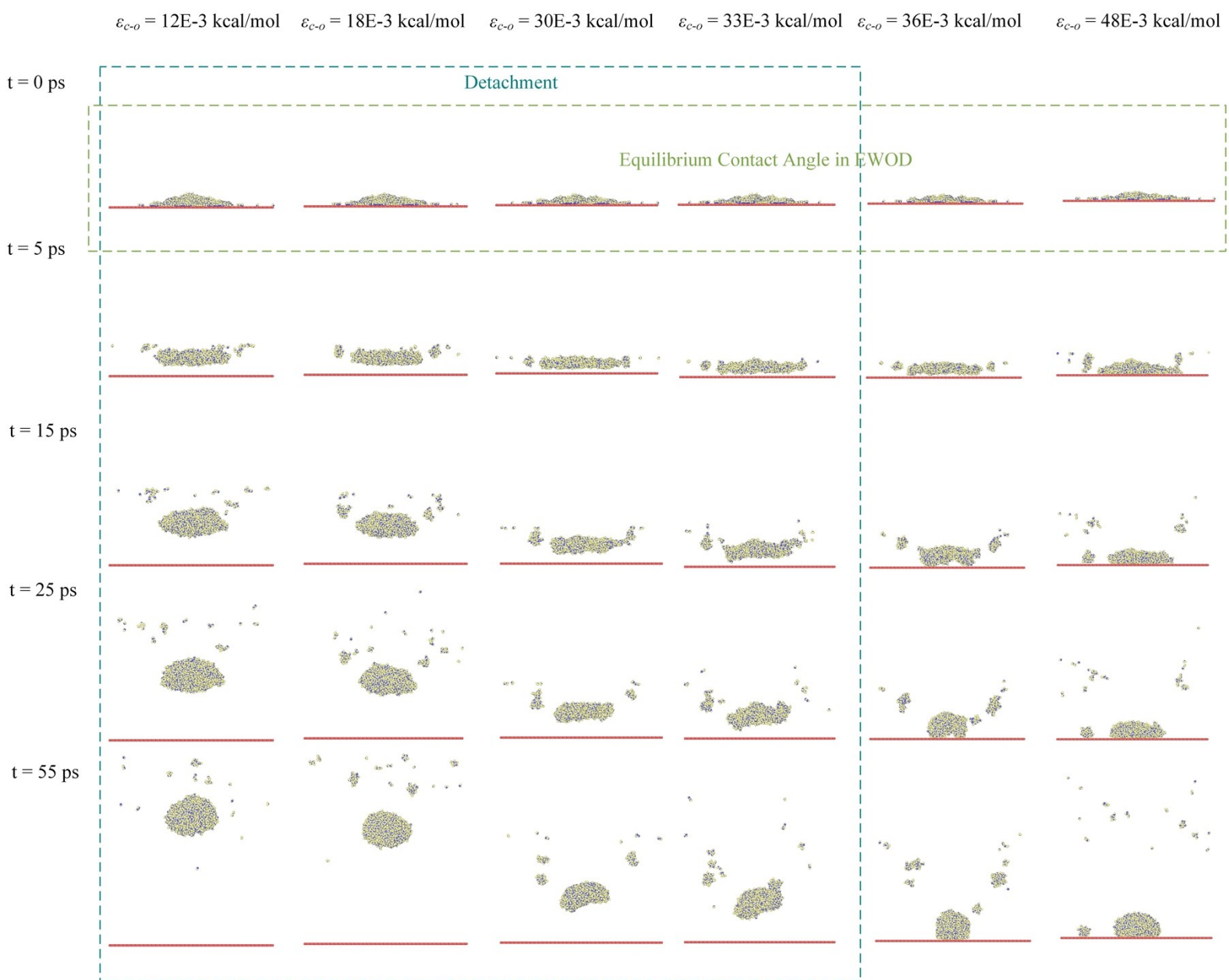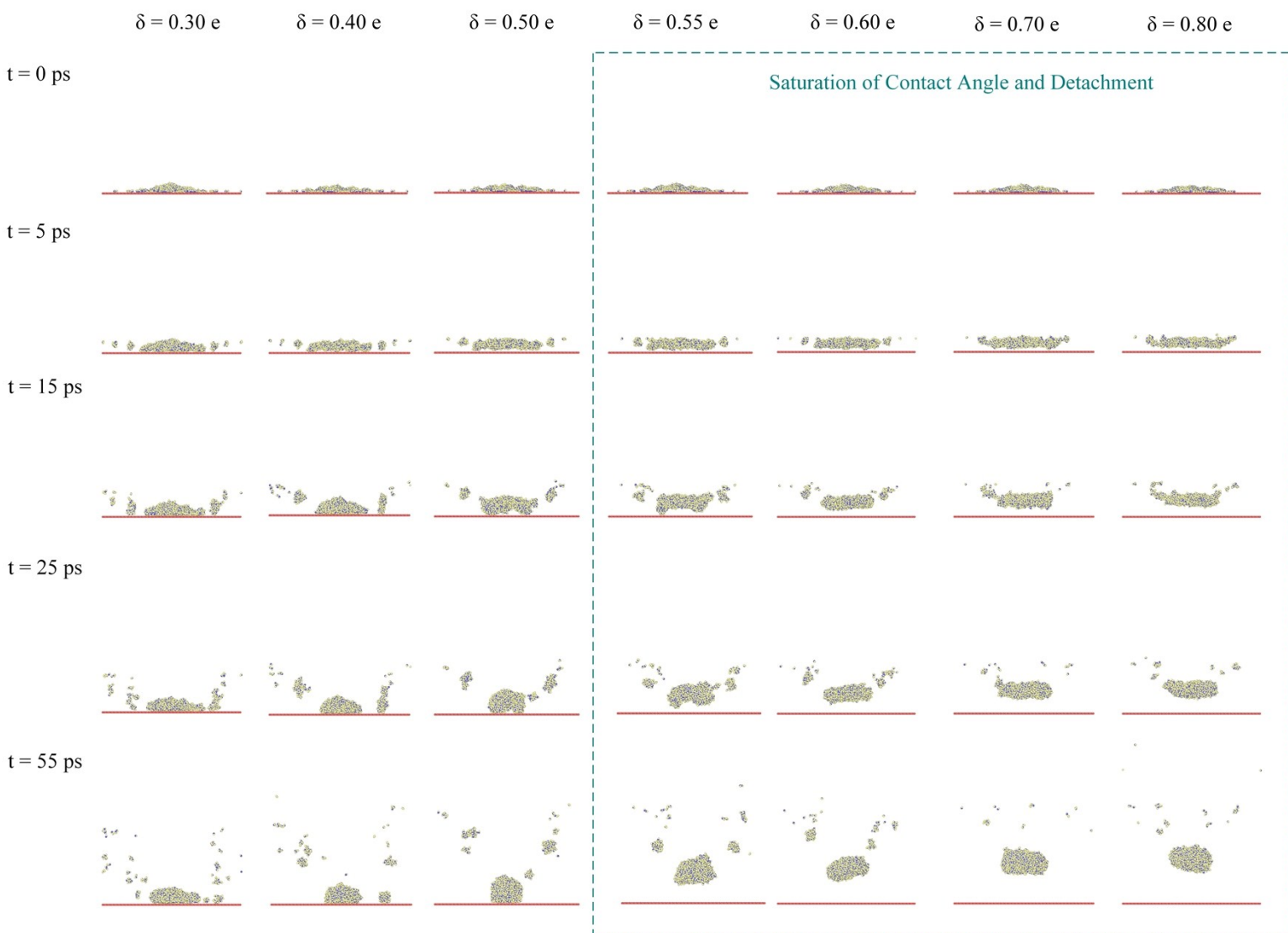
Fig.S2. Screen shots of droplet movement after removing the E-field with variation in the initial wettability. (Corresponding to Fig.3d to e)

4. Observation of droplet detachment with increase of *E*-field at ε_{c-o} = 36E-3 kcal/mol

Fig.S3 shows the screen shots of droplet movement after removing the E-field for ε_{c-o} = 36E-3 kcal/mol, which corresponds to Fig.4b. It is seen that the droplet jumps off for all $\delta \geq 0.55$ *e*, indicating that one is able to activate a droplet on a more hydrophilic surface by increasing the *E*-field. In addition, the critical δ increases with

increase of initial wettability ($\varepsilon_{c\text{-}o}$) while the velocity of droplet decreases when compared with $\varepsilon_{c\text{-}o}$ = 12E-3 kcal/mol (Fig.S2).


Fig.S3. Screen shots of droplet movement after removing the E-field with variation in the E-field and $\varepsilon_{c\text{-}o}$ = 36E-3kcal/mol . (Corresponding to Fig.4b)

5. Gouy-Chapman-Stern model for EDL

The Gouy-Chapman-Stern model defines three regions in the EDL, i.e., the diffusion layer, outer Stern layer and inner Stern layer. The diffusion layer is beyond the shear plane with the potential of ζ, where the potential decreases expontially. In this region, the ions are less affected by the surface charges. The outer Stern layer exists between the outer Helmholtz plane (OHP with potential of ψ_{OHP}) and inner Helmholtz plane (IHP with potential of ψ_{IHP}). In this layer, the ions are hydrated and

the potential decreases linearly. Close to the IHP, the ions are not hydrated, and beyond it, there is no molecules and the potential increases away from the surface. To penetrate into the IHP, the molecules has to overcome the potential well (ψ_{IHP} - ψ_S).
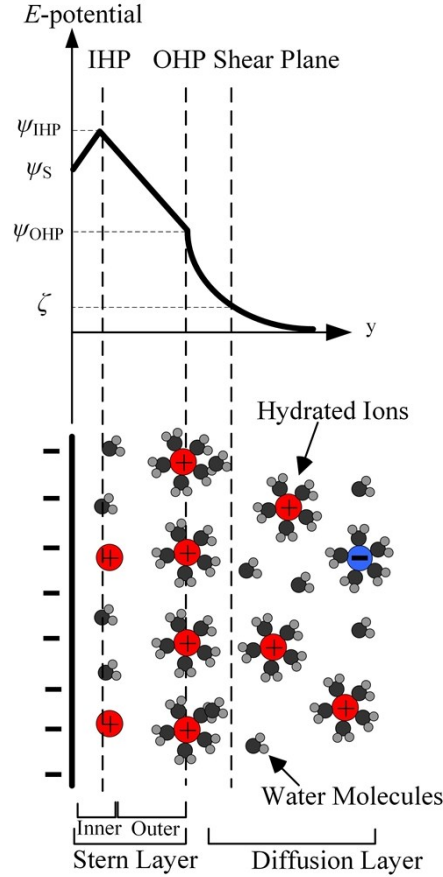

Figure.S4. Gouy-Chapman-Stern Model

6. Validation of Simulation Model

In order to exclude the effect of droplet size (number of water molecules) and span of strip-electrode, the contact angles at EWOD state and the movement of droplet after removal of E-field for the cases with different simulation configurations are provided.

Fig.S5 compares the equilibrium contact angle at EWOD state with different charges when using 2000 and 4000 water molecules with the span of strip 17 Å (ε_{c-o} = 12E-3 kcal/mol). The upper two rows display the droplets of 4000 water molecules. It is seen that the saturated contact angles are slightly different for two-cases. However, the transition charge density (0.15 e) is also similar for two cases. More importantly, in both cases, the droplet can only be actuated after the saturation of contact angle.

The above results indicate that 2000 water molecules are sufficient for this study.
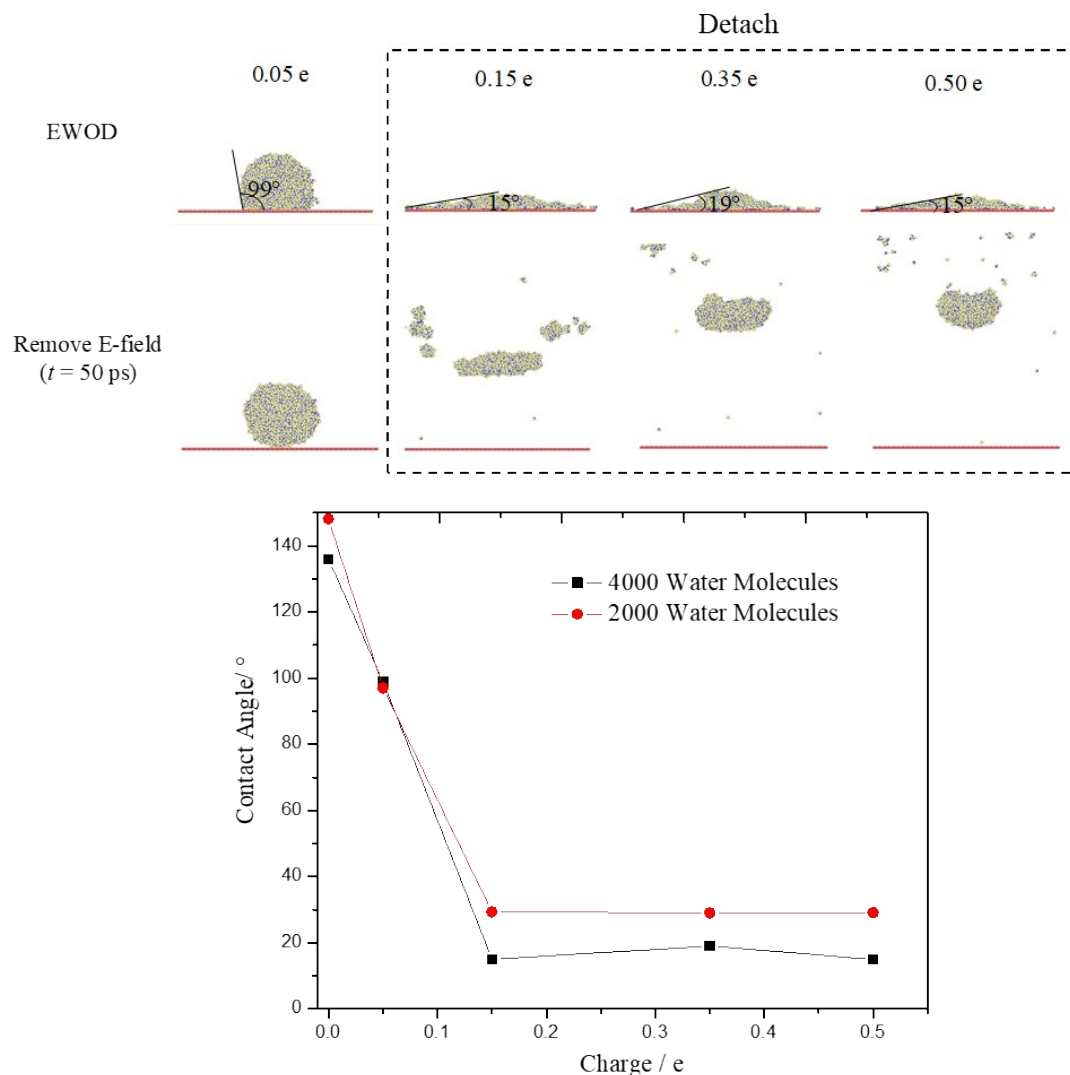
Figure.S5. Effect of droplet size on contact angle at EWOD state and droplet-movement after removal of E-field.

Fig.S6 compares the equilibrium contact angle at EWOD state with different charges using the strip-electrode with span of 17 Å and 8.5 Å with 2000 water molecules ($\varepsilon_{c\text{-}o}$ = 12E-3 kcal/mol). The upper two rows display the droplets when the 8.5 Å strip-electrode is used. It is seen that the span of strip-electrode slightly affects the value of saturated contact angle. However, it does not affect the transition magnitude of E-field (0.15e).
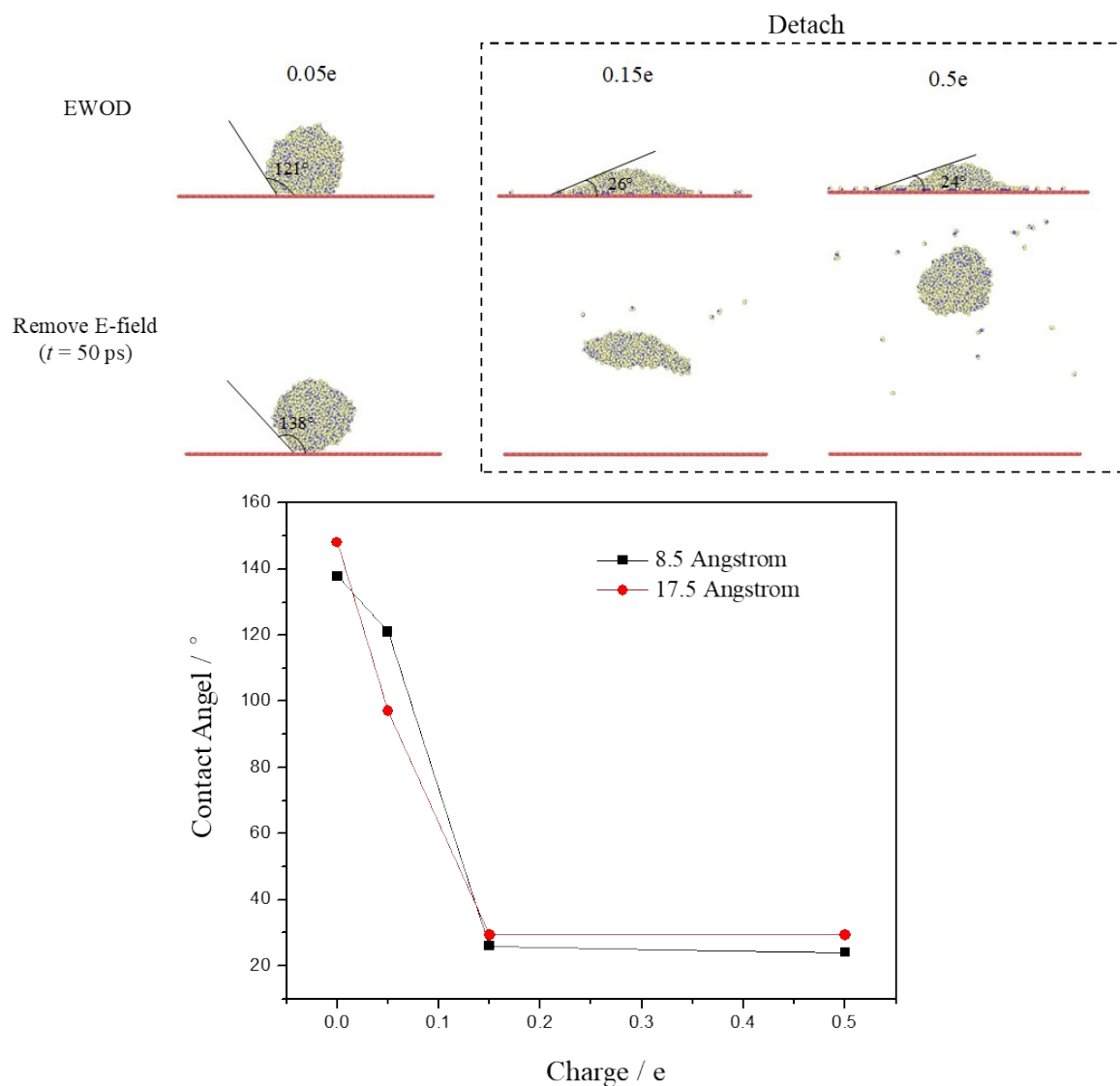
Figure.S6. Effect of span of strip-electrode on contact angle at EWOD state and droplet-movement after removal of E-field.

7. Videos

See attachments for the videos with the conditions below:

A: Electrowetting process for ε_{c-o} = 12E-3 kcal/mol and δ = 0.05 e

B: Detachment process for ε_{c-o} = 12 E-3 kcal/mol and δ = 0.05 e

C: Electrowetting process for ε_{c-o} = 12E-3 kcal/mol and δ = 0.5 e

D: Detachment process for ε_{c-o} = 12E-3 kcal/mol and δ = 0.5 e

E: Electrowetting process for ε_{c-o} = 36E-3 kcal/mol and δ = 0. 5 e

F: Detachment process for ε_{c-o} = 36E-3 kcal/mol and δ = 0. 5e

G: Electrowetting process for ε_{c-o} = 36E-3 kcal/mol and δ = 0.8 e

H: Detachment process for ε_{c-o} = 36E-3 kcal/mol and δ = 0.8 e

References

1.   Oldham, K. B. *J Electroanal Chem* **2008,** 613, (2), 131-138.

2.   Quinn, A.; Sedev, R.; Ralston, J. *The journal of physical chemistry B* **2005,** 109, (13), 6268-6275.

3.   Chandra, S.; Avedisian, C. In *On the collision of a droplet with a solid surface*, Proc. R. Soc. Lond. A, 1991; The Royal Society: pp 13-41.

4.   Ashgriz, N.; Movassat, M., Oscillation of droplets and bubbles. In *Handbook of Atomization and Sprays*, Springer: 2011; pp 125-144.

5.   Zisman, W. A., Relation of the equilibrium contact angle to liquid and solid constitution. ACS Publications: 1964.